Ubiquitous production of branched glycerol dialkyl glycerol tetraethers (brGDGTs) in global marine environments: a new source indicator for brGDGTs

Wenjie Xiao[1,2], Yinghui Wang[2], Shangzhe Zhou[2], Limin Hu[3], Huan Yang[4], Yunping Xu[1,2*]

[1]Shanghai Engineering Research Center of Hadal Science and Technology, College of Marine Sciences, Shanghai Ocean University, Shanghai 201306, China
[2]MOE Key Laboratory for Earth Surface Process, College of Urban and Environmental Sciences, Peking University, Beijing 100871, China
[3]Key Laboratory of Marine Sedimentology and Environmental Geology, First Institute of Oceanography, State Oceanic Administration, Qingdao 266061, China
[4]State Key Laboratory of Biogeology and Environmental Geology, China University of Geosciences, Wuhan 430074, China
Corresponding author: Y Xu (ypxu@shou.edu.cn)

Abstract. Presumed source specificity of branched glycerol dialkyl glycerol tetraethers (brGDGTs) from bacteria thriving in soil/peat and isoprenoid GDGTs (iGDGTs) from aquatic organisms led to the development of several biomarker proxies for biogeochemical cycle and paleoenvironment. However, recent studies reveal that brGDGTs are also produced in aquatic environments besides soils and peat. Here we examine three cores from the Bohai Sea and found distinct difference in brGDGT compositions varying with the distance from the Yellow River mouth. We thus propose an abundance ratio of hexamethylated to pentamethylated brGDGT (IIIa/IIa) to evaluate brGDGT sources. The compilation of globally distributed 1354 marine sediments and 589 soils shows that the IIIa/IIa ratio is generally <0.59 in soils, 0.59–0.92 and >0.92 in marine sediments with and without significant terrestrial inputs, respectively. Such disparity confirms the existence of two sources for brGDGTs, a terrestrial origin with lower IIIa/IIa and a marine origin with higher IIIa/IIa, which is likely attributed to generally higher pH and the production of brGDGTs in cold deep

water in sea. The application of the IIIa/IIa ratio to the East Siberian Arctic Shelf proves it a sensitive source indicator for brGDGTs, which is helpful for accurate estimation of organic carbon source and paleoclimates in marine settings.

1 Introduction

Glycerol dialkyl glycerol tetraethers (GDGTs), membrane lipids of archaea and certain bacteria, are widely distributed in marine and terrestrial environments (Reviewed by Schouten et al., 2013). These lipids have been a focus of attention of organic geochemists for more than ten years because they can be used to estimate environmental variables in the past such as temperature, soil pH, organic carbon source and microbial community structure (e.g., Schouten et al., 2002; Hopmans et al., 2004; Weijers et al., 2006; Lipp et al., 2008; Kim et al., 2010; Peterse et al., 2012; Zhu et al., 2016). There are generally two types of GDGTs, isoprenoid (iGDGTs) and non-isoprenoid, branched GDGTs (brGDGTs; Fig. 1). The former group is more abundant in aquatic settings and generally thought to be produced by Thaumarchaeota, a specific genetic cluster of the archaea domain (Sinninghe Damsté et al., 2002; Schouten et al., 2008), although Euryarchaeota may be a significant source of iGDGTs in the ocean (e.g., Lincoln et al., 2014). In contrast, the 1,2-di-*O*-alkyl-*sn*-glycerol configuration of brGDGTs was interpreted as an evidence for a bacterial rather than archaeal origin for brGDGTs (Sinninghe Damsté et al., 2000; Weijers et al., 2006). So far, only one brGDGT with two 13,16-dimethyl octacosanyl moieties was unambiguously detected in two species of Acidobacteria (Sinninghe Damsté et al., 2011), which hardly explains high diversity and ubiquitous occurrence of up to 15 brGDGT isomers in environments (Weijers et al., 2007b; De Jonge et al., 2014). Therefore, other biological sources of brGDGTs, although not yet identified, are likely.

The source difference between brGDGTs and iGDGTs led researchers to developing a branched and isoprenoid tetraether (BIT) index, expressed as relative abundance of terrestrial-derived brGDGTs to aquatic-derived Thaumarchaeota (Hopmans et al., 2004). Subsequent studies found that the BIT index is specific for soil

organic carbon because GDGTs are absent in vegetation (e.g., Walsh et al., 2008; Sparkes et al., 2015). The BIT index is generally higher than 0.9 in soils, but close to 0 in marine sediments devoid of terrestrial inputs (Weijers et al., 2006; Weijers et al., 2014). Since its advent, the BIT index has been increasingly used to trace soil organic matter in different environments (e.g., Herfort et al., 2006; Kim et al., 2006; Blaga et al., 2011; Loomis et al., 2011; Wu et al., 2013). However, the BIT index is not just dependent on the abundance of brGDGTs, which reflects the input of soil organic matter, but also on the abundance of crenarchaeol, which is linked to marine productivity (e.g., Herfort et al., 2006; Smith et al, 2012; Fietz et al., 2012). Besides the BIT index, Weijers et al. (2007b) found that the number of cyclopentane moieties of brGDGTs, expressed as Cyclization of Branched Tetraethers (CBT), correlated negatively with soil pH, while the number of methyl branches of brGDGTs, expressed as Methylation of Branched Tetraethers (MBT), was dependent on annual mean air temperature (MAT) and to a lesser extent on soil pH. The MBT/CBT proxies were further corroborated by subsequent studies (e.g., Sinninghe Damsté et al., 2008; Peterse et al., 2012; Yang et al., 2014a). Assuming that brGDGTs preserved in marine sediments close to the Congo River outflow were derived from soils in the river catchment, Weijers et al. (2007a) reconstructed large-scale continental temperature changes in tropical Africa that span the past 25,000 years by using the MBT/CBT proxy. Recently, De Jonge et al. (2013) used a tandem high performance liquid chromatography-mass spectrometry (2D HPLC-MS) and identified a series of novel 6-methyl brGDGTs which were previously coeluted with 5-methyl brGDGTs. This finding resulted in the redefinition and recalibration of brGDGTs' indexes (e.g., De Jonge et al., 2014; Xiao et al., 2015).

One underlying assumption of all brGDGT-based parameters is their source specificity, i.e., brGDGTs is only biosynthesized by bacteria thriving in soils and peat. Several studies, however, observed different brGDGT compositions between marine sediments and soils on adjacent lands, supporting in situ production of brGDGTs in marine environments (e.g., Peterse et al., 2009a; Zhu et al., 2011; Liu et al., 2014; Weijers et al., 2014; Zell et al., 2014), analogous to lacustrine settings (e.g., Sinninghe Damsté et al., 2009; Tierney & Russell, 2009; Tierney et al., 2012) and rivers (e.g., Zhu

et al., 2011; De Jonge et al., 2015; French et al., 2015; Zell et al., 2015). Peterse et al. (2009) compared the brGDGTs' distribution in Svalbard soils and nearby fjord sediments, and found that concentrations of brGDGTs (0.01–0.20 μg/g dw) in fjord sediments increased towards the open ocean and the distribution was strikingly different from that in soil. Zhu et al. (2011) examined distributions of GDGTs in surface sediments across a Yangtze River-dominated continental margin, and found evidence for production of brGDGTs in the oxic East China Sea shelf water column and the anoxic sediments/waters of the Lower Yangtze River. At the global scale, Fietz et al. (2012) reported a significant correlation between concentrations of brGDGTs and crenarchaeol ($p < 0.01$; $R^2 = 0.57–0.99$), suggesting that a common or mixed source for brGDGTs and iGDGTs are actually commonplace in lacustrine and marine settings. More recently, Sinninghe Damsté (2016) reported tetraethers in surface sediments from 43 stations in the Berau River delta (Kalimantan, Indonesia), and this result, combined with data from other shelf systems, are coherent with the hypothesis that brGDGTs are in situ produced in shelf sediments especially at water depth of 50–300 m.

Fluvial inputs and wind are the most important pathways for transporting terrestrial material into sea. In continental shelf, fluvial discharge is more important because brGDGTs in atmospheric dust are either below the detection level (Hopmans et al., 2004) or present at low abundance (Fietz et al., 2013; Weijers et al., 2014). In the remote ocean where no direct impact from land erosion via rivers takes place, eolian transport and in situ production are major contributors for brGDGTs. Weijers et al. (2014) found that distributions of African dust-derived brGDGTs were similar to those of soils but different from those of distal marine sediments, providing a possibility to distinguish terrestrial vs. marine brGDGTs based on molecular compositions. However, so far no robust molecular indicator is available for estimating source of brGDGTs in marine environments. Considering this, we conduct a detailed study about GDGTs in three cores from the Bohai Sea which are subject to the Yellow River influence to different degree. Our purpose is to evaluate the source discerning capability of different brGDGT parameters, from which the most sensitive parameter is selected and applied

for globally distributed marine sediments and soils to test whether it is valid at the global scale. Our study supplies an important step for improving accuracy of brGDGT-derived proxies and better understanding marine carbon cycle and paleoenvironments.

2 Material and methods

2.1 Study area and sampling

The Bohai Sea is a semi-enclosed shallow sea in northern China, extending about 550 km from north to south and about 350 km from east to west. Its area is 77,000 km^2 and the mean depth is 18 m (Hu et al., 2009). The Bohai Strait at the eastern portion is the only passage connecting the Bohai Sea to the outer Yellow Sea. Several rivers, including Yellow River, the second largest river in the world in terms of sediment load (Milliman & Meade, 1983), drain into the Bohai Sea with a total annual runoff of 890×10^8 m^3. A 64 cm long gravity core (M1; 37.52°N, 119.32°E) was collected in July 2011, while other two cores, M3 (38.66°N, 119.54°E; 53 cm long) and M7 (39.53°N, 120.46°E; 60 cm long), were collected in July 2013 (Fig. 2). The sites M1, M3 and M7 are located in the south, the center and the north of the Bohai Sea, respectively. The cores were transported to the lab where they were sectioned at 1 or 2 cm interval. The age model was established on basis of ^{210}Pb and ^{137}Cs activity, showing that the bottom sediments are less than 100 years old (Wu et al., 2013 and unpublished data).

2.2 Lipid extraction and analyses

The detailed procedures for lipid extraction and GDGT analyses have been described in previous studies (Ding et al., 2015; Xiao et al., 2015). Briefly, the homogenous freeze-dried samples were ultrasonically extracted with dichloromethane (DCM)/methanol (3:1 v:v). The extracts were separated into nonpolar and polar fraction over silica gel columns. The latter fraction containing GDGTs was analyzed using an Agilent 1200 HPLC-atmospheric pressure chemical ionization-triple quadruple mass spectrometry (HPLC-APCI-MS) system. The separation of 5- and 6-methyl brGDGTs was achieved with two silica columns in sequence (150 mm×2.1 mm; 1.9 μm, Thermo Finnigan; USA). The quantification was achieved by comparison of the respective

protonated ion peak areas of each GDGT to the internal standard (C_{46} GDGT) in selected ion monitoring (SIM) mode. The protonated ions were m/z 1050, 1048, 1046, 1036, 1034, 1032, 1022, 1020, 1018 for brGDGTs, 1302, 1300, 1298, 1296, 1292 for iGDGTs and 744 for C_{46} GDGT.

2.3 Parameter calculation and statistics

The BIT, MBT, Methyl Index (MI), Degree of Cyclization (DC) of brGDGTs and weighted average number of cyclopentane moieties for tetramethylated brGDGTs ($\#Rings_{tetra}$) were calculated according to the definitions of Hopmans et al. (2004), Weijers et al. (2007b), Zhang et al. (2011), Sinninghe Damsté et al. (2009) and Sinninghe Damsté (2016), respectively.

$$BIT = \frac{Ia + IIa + IIIa}{Ia + IIa + IIIa + IV} \quad (1)$$

$$MBT = \frac{Ia + Ib + Ic}{Ia + IIa + IIIa + Ib + IIb + IIIb + Ic + IIc + IIIc} \quad (2)$$

$$MI = 4 \times (Ia + Ib + Ic) + 5 \times (IIa + IIb + IIb) + 6 \times (IIIa + IIIb + IIIc) \quad (3)$$

$$DC = \frac{Ib + IIb}{Ia + IIa + Ib + IIb} \quad (4)$$

$$\#Rings_{tetra} = \frac{Ib + 2 \times Ic}{Ia + Ib + Ic} \quad (5)$$

where roman numbers denote relative abundance of compounds depicted in Fig. 1. In this study, we used two silica LC columns in tandem and successfully separated 5- and 6-methyl brGDGTs. However, many previous studies (e.g., Weijers et al., 2006) used one LC column and did not separate 5- and 6-methyl brGDGTs. Considering this, we combined 5-methyl and 6-methyl brGDGT as one compound in this study, for example, IIIa denotes the total abundance of brGDGT IIIa and IIIa' in figure 1.

An analysis of variance (ANOVA) was conducted for different types of samples to determine if they differ significantly from each other. The SPSS 16.0 software package (IBM, USA) was used for the statistical analysis. Squared Pearson correlation coefficients (R^2) were reported and a significance level is $p < 0.05$.

2.4 Data compilation of global soils and marine sediments

The dataset in this study are composed of relative abundance of GDGTs and derived parameters from 1354 globally distributed soils and 589 marine sediments (Fig. 2 and supplementary data). These sampling sites span a wide area from 75.00°S to 79.28°N and 168.08°W to 174.40°E and the water depth ranges from 1.0 to 5521 m. The marine samples are from the South China Sea (Hu et al., 2012; Jia et al., 2012; O'Brien et al., 2014; Dong et al., 2015), Caribbean Sea (O'Brien et al., 2014), western equatorial Pacific Ocean (O'Brien et al., 2014), southeast Pacific Ocean (Kaiser et al., 2015), the Chukchi and Alaskan Beaufort Seas (Belicka & Harvey, 2009), eastern Indian Ocean (Chen et al., 2014), East Siberian Arctic Shelf (Sparkes et al., 2015), Kara Sea (De Jonge et al., 2015; De Jonge et al., 2016), Svalbard fjord (Peterse et al., 2009a), Red Sea (Trommer et al., 2009), the southern Adriatic Sea (Leider et al., 2010), Columbia estuary (French et al., 2015), globally distributed distal marine sediments (Weijers et al., 2014) and the Bohai Sea (this study). Soil samples are from the Svalbard (Peterse et al., 2009b), Columbia (French et al., 2015), China (Yang et al., 2013; Yang et al., 2014a; Yang et al., 2014b; Ding et al., 2015; Xiao et al., 2015; Hu et al., 2016), globally distributed soils (Weijers et al., 2006; Peterse et al., 2012; De Jonge et al., 2014), California geothermal (Peterse et al., 2009b), France and Brazil (Huguet et al., 2010), western Uganda (Loomis et al., 2011), the USA (Tierney et al., 2012), Tanzania (Coffinet et al., 2014), Indonesian, Vietnamese, Philippine, China and Italia (Mueller-Niggemann et al., 2016).

3 Results and discussion

3.1 Distribution and source of brGDGTs in Bohai Sea

A series of iGDGTs including crenarchaeol and brGDGTs including 5-methyl and 6-methyl isomers were detected in Bohai Sea sediments. For brGDGTs, a total of 15 compounds were identified including three tetramethylated brGDGTs (Ia, Ib and Ic), six pentamethylated brGDGTs (IIa, IIb, IIc, IIa', IIb' and IIc') and six hexamethylated brGDGTs (IIIa, IIIb, IIIc, IIIa', IIIb' and IIIc'). In order to evaluate provenances of brGDGTs, we calculated various parameters including the BIT index, percentages of tetra-, penta- and hexa-methylated brGDGTs, #rings for tetramethylated brGDGTs, DC,

MI, MBT, brGDGTs IIIa/IIa and Ia/IIa (Table 1). The value of the BIT index ranged from 0.27 to 0.76 in the core M1, which is much higher than that in the core M3 (0.04–0.25) and the core M7 (0.04–0.18). Such difference is not surprising since the site M1 is closest to the Yellow River outflow, and receives more terrestrial organic carbon than other two sites (Fig. 2). However, the BIT index itself has no ability to determine the source of brGDGTs (terrestrial vs. aquatic) because brGDGTs and crenarchaeol used in this index are thought to be specific for soil organic carbon and marine organic carbon, respectively (Hopmans et al., 2004), although crenarchaeol is also present in soils at low abundance (Weijers et al., 2006). For individual brGDGTs, the core M1 is characterized by significantly higher percentage of brGDGT IIa (28±1%) than the core M2 (18±1%) and the core M3 (18±0%; Fig. 3). We performed ANOVA for a variety of brGDGTs' parameters. All results except from MI show a significant difference between Chinese soils and Bohai Sea sediments. The IIIa/IIa ratio is the most sensitive parameter which can completely separate the samples into four groups: Chinese soils (0.39±0.25; Mean±SD; same hereafter), M1 sediments (0.63±0.06), M3 sediments (1.16±0.12) and M7 sediments (0.93±0.07).

Three factors may account for the occurrence of higher IIIa/IIa ratio in the Bohai Sea sediments than Chinese soils: selective degradation during land to sea transport, admixture of river produced brGDGTs and in situ production of brGDGTs in sea. Huguet et al. (2008; 2009) reported that iGDGTs (i.e., crenarchaeol) was degraded at a rate of 2-fold higher than soil derived brGDGTs under long term oxygen exposure in the Madeira Abyssal Plain, leading to increase of the BIT index. Such selective degradation, however, cannot explain significant different IIIa/IIa ratio between the Chinese soils and Bohai Sea sediments because unlike crenarchaeol, both IIIa and IIa belong to brGDGTs with similar chemical structures and thus have similar degradation rates. In situ production of brGDGTs in rivers is a widespread phenomenon, and can change brGDGTs' composition in sea when they were transported there (e.g., Zhu et al., 2011; De Jonge et al., 2015; Zell et al., 2015). However, this effect is minor in the Yellow River because extremely high turbidity (up to 220 kg/m^3 during the flood season; Ren & Shi, 1986) greatly constrain the growth of aquatic organisms. The studies along

lower Yellow River-estuary-coast transect suggested that brGDGTs in surface sediments were primarily a land origin (Wu et al., 2014). In our study, the site M1 is adjacent to the Yellow River mouth and receives the largest amount of terrestrial organic matter, causing lower IIIa/IIa values (0.63±0.06). In contrast, the site M3 located in central Bohai Sea comprises of the least amount of terrestrial organic matter, resulting in higher IIIa/IIa values (1.16±0.12). The intermediate IIIa/IIa value at the site M7 (0.93±0.07) is attributed to moderate land erosion nearby northern Bohai Sea (Fig. 2). These results, consistent with other terrestrial biomarkers such as C_{29} and C_{31} *n*-alkanes and C_{29} sterol (unpublished data), suggest that the higher IIIa/IIa values in the Bohai Sea sediments compared to Chinese soils (0.39±0.25) is most likely caused by in situ production of brGDGTs.

3.2 Regional and global validation of brGDGT IIIa/IIa

To test whether the IIIa/IIa ratio is valid in other environments, we apply it to the Svalbard (Peterse et al., 2009a), the Yenisei River outflow (De Jonge et al., 2015) and the East Siberian Arctic Shelf (Sparkes et al., 2015). Similar to Bohai Sea, the brGDGT IIIa and IIa are also ubiquitously present in these environments. By comparing the compositions of brGDGTs in Svalbard soils and nearby fjord sediments, Peterse et al. (2009a) indicated that sedimentary organic matter in fjords was predominantly a marine origin. A plot of BIT vs. IIIa/IIa (Fig. 4a) clearly grouped the samples into two groups which correspond to soils (>0.75 for BIT and <1.0 for IIIa/IIa) and marine sediments (<0.3 for BIT and >1.0 for IIIa/IIa). Another line of evidence is from De Jonge et al. (2015) who examined brGDGTs in core lipids (CLs) and intact polar lipids (IPLs) in the Yenisei River outflow. As the IPLs are rapidly degraded in the environment, they can be used to trace living or recently living material, while the CLs are generated via degradation of the IPLs after cell death (White et al., 1979; Lipp et al., 2008). The compilation of brGDGTs' abundance from De Jonge et al. (2015) shows significant difference of the IIIa/IIa ratio between the IPL fractions (>1.0) and CL fractions (<0.8; Fig. 4b). Such disparity supports that brGDGTs produced in marine environments have

higher IIIa/IIa values because labile intact polar brGDGTs are mainly produced in situ, whereas recalcitrant core brGDGTs are composed of more allochthonous terrestrial components. Sparkes et al. (2015) examined brGDGTs in surface sediments across the East Siberian Arctic Shelf (ESAS) including the Dmitry-Laptev Strait, Buor-Khaya Bay, ESAS nearshore and ESAS offshore. The plot of BIT vs. IIIa/IIa again results into two groups, one group with lower BIT values (<0.3) and higher IIIa/IIa values (0.8–2.3) mainly from ESAS offshore, and another group with higher BIT values (0.3–1.0) and lower IIIa/IIa values (0.4–0.9) from the Dmitry-Laptev Strait, Buor-Khaya Bay and ESAS nearshore (Fig. 4c). A strong linear correlation was observed between the IIIa/IIa ratio and the distance from river mouth (R^2=0.58; p<0.05; Fig. 4d), in accord with the data of the BIT index and $\delta^{13}C_{org}$ (Sparkes et al., 2015). All lines of evidence support that marine-derived brGDGTs have higher IIIa/IIa values than terrestrial derived brGDGTs.

We further extend the dataset on global scale (Fig. 5), showing that the IIIa/IIa ratio is still significantly higher in marine sediments than soils ($p < 0.01$). An exception was observed for Red Sea sediments which have unusually low IIIa/IIa values (0.39±0.21) compared to other marine sediments (>0.87). The Red Sea has a restricted connection to the Indian Ocean via the Bab el Mandeb Strait. This, combined with high insolation, low precipitation and strong winds result in surface water salinity up to 41 in the south and 36 in the north of the Red Sea (Sofianos et al., 2002). Under such extreme environment, distinct microbial populations may be developed and produced GDGTs different from that in other marine settings (See Trommer et al., 2009 for details).

Overall, the global distribution of IIIa/IIa presents the highest values in many deep sea sediments (2.6–5.1), the lowest values in soils (<1.0), and intermediate values in sediments from bays, coastal areas or marginal seas (0.87–2.62; Fig. 5). These results are consistent with our data from the Bohai Sea, and confirm that the IIIa/IIa ratio is a useful proxy for tracing the source of brGDGTs in marine sediments at regional and global scales.

Why do marine sediments generally have higher IIIa/IIa values than soils? It has

been reported that relative number of methyl groups positively correlates with soil pH and negatively correlates with MAT (Weijers et al., 2007b; Peterse et al., 2012). The IIIa/IIa ratio is actually an abundance ratio of hexamethylated to pentamethylated brGDGT, and thus is also affected by ambient temperature and pH. Unlike iGDGTs which is well known to be mainly produced by Thaumarchaeota (Sinninghe Damsté et al., 2002; Schouten et al., 2008), the marine source of brGDGTs remains elusive. Here, we assume that marine organisms producing brGDGTs response to ambient temperature in the same way as those soil bacteria producing brGDGTs, i.e., a negative correlation between relative number of methyl group of brGDGTs and ambient temperature. Because a large temperature gradient exists from surface to bottom water in ocean, we need consider the locale where brGDGTs are produced. If brGDGTs in marine environments are predominantly produced in euphotic zone, we would not observe a significant difference for the IIIa/IIa ratio between land and sea because both soils and marine sediments are globally distributed, leading to no systematic difference between soil temperature and sea surface temperature. Alternatively, if brGDGTs in marine sediments are partially derived from deep-water dwelling or benthic organisms, cold deep water (generally 1–2 ^{o}C) would cause higher IIIa/IIa values in marine sediments, as we observed in this study. Although to the best of our knowledge, there is no study reporting in situ production of brGDGTs throughout water column in ocean. Recent studies (Taylor et al., 2013; Kim et al., 2015) have suggested that Thaumarchaeota thriving in the deeper, bathypelagic water-column (>1000 m water depth) biosynthesized iGDGTs with different compositions as surface dwelling Thaumarchaeota, and thereby alter signals of TEX_{86} in sediments. Besides temperature, pH can also alter compositions of brGDGTs (Weijers et al., 2007). Based on global soil data, the IIIa/IIa ratio shows a strong positive correlation with soil pH (R^2=0.51; Fig. 6). In our study, the majority of soils are acidic or neutral (pH<7.3) and only 8% of soil samples mainly from semi-arid and arid regions have pH of >8.0 (e.g., Yang et al., 2014a). In contrast, seawater is constantly alkaline with a mean pH of 8.2. With this systematic difference, bacteria living in soils tend to produce higher proportions of brGDGT IIa, whereas unknown marine organisms tend to biosynthesize higher

proportions of brGDGT IIIa if they response to ambient pH in a similar way as soil bacteria in term of biosynthesis of brGDGTs. It should be pointed out that unlike fairly stable pH of overlying sea water, the pH of pore waters in marine sediments can vary significantly, which may influence compositions of brGDGTs. Nevertheless, at current stage, the occurrence of higher IIIa/IIa values in marine sediments is most likely attributed to relatively higher pH and lower deep water temperature. Further studies are needed to disentangle relative importance of these two factors.

3.3 Implication of IIIa/IIa on other brGDGT proxies

Because brGDGTs can be produced in marine settings, they are no longer specific for soil organic matter, which inevitably affects brGDGT-derived proxies (e.g., BIT, MBT/CBT). The plot of BIT vs. IIIa/IIa on basis of global dataset shows that the IIIa/IIa ratio has the value of <0.59 for 90% of soil samples and >0.92 for 90% of marine sediments (Fig. 7). Considering this fact, we propose that the IIIa/IIa ratio of <0.59 and >0.92 represents terrestrial (or soil) and marine endmembers, respectively. The BIT index has the value of >0.67 for 90% of soils and <0.16 for 90% of marine sediments (Fig. 7). Overall, the BIT index decreased with increasing IIIa/IIa values($\mathrm{BIT} = 1.08 \times 0.28^{\frac{\mathrm{IIIa}}{\mathrm{IIa}}} - 0.03; \mathrm{R}^2 = 0.77$; Fig. 7), suggesting that both the IIIa/IIa and BIT are useful indexes for assessing soil organic carbon in marine settings. However, when the BIT index has an intermediate value (i.e., 0.16 to 0.67), it is not valid to determine the provenance of brGDGTs. For example, several marine samples having BIT values of ~0.35 show a large range of IIIa/IIa (0.4 to 2.4; Fig. 7), suggesting that the source of brGDGTs can vary case by case. Under this situation, the calculation of the IIIa/IIa ratio is strongly recommended.

The different IIIa/IIa values between land and marine endmembers may supply an approach to quantify the contribution of soil organic carbon in marine sediments. Similar to the BIT index, we used a binary mixing model to calculate percentage of soil organic carbon ($\%OC_{soil}$) as follow:

$$\%OC_{soil} = \left[\frac{[IIIa/IIa]_{sample} - [IIIa/IIa]_{marine}}{[IIIa/IIa]_{soil} - [IIIa/IIa]_{marine}}\right] * 100 \qquad (6)$$

Where $[IIIa/IIa]_{sample}$, $[IIIa/IIa]_{soil}$ and $[IIIa/IIa]_{marine}$ are the abundance ratio of brGDGT IIIa/IIa for samples, soils and marine sediments devoid of terrestrial influences, respectively.

We applied this binary mixing model to the East Siberian Arctic Shelf because the data of BIT, $\delta^{13}C_{org}$ and distance from river mouth are all available (Sparkes et al., 2015). With the distance from river mouth increasing from 25 to >700 km, the BIT, IIIa/IIa and $\delta^{13}C_{org}$ change from 0.95 to 0, 0.53 to 2.21 and –27.4‰ to –21.2‰, respectively, reflecting spatial variability of sedimentary organic carbon sources. For the BIT index, we used 0.97 and 0.01 as terrestrial and marine endmember values based on previous studies for Arctic surrounding regions (De Jonge et al., 2014; Peterse et al., 2014), which are similar to global average values (Hopmans et al., 2004). For $\delta^{13}C_{org}$, we chose –27‰ and –20‰ as C3 terrestrial and marine organic carbon endmembers (Meyers, 1997). For the IIIa/IIa ratio, we used a global average value of marine sediments (1.6) and soils (0.24), respectively, based on this study. By applying these endmember values into Eq. 6, we calculated percentage of soil organic carbon ($\%OC_{soil}$). We removed a few data points if their calculated $\%OC_{soil}$ were greater than 100% or below 0%. It should be noted that the endmember value will affect quantitative results, but does not change a general trend of $\%OC_{soil}$. The results based on all three parameters show a decreasing trend seawards (Fig. 8). However, the $\%OC_{soil}$ based on $\delta^{13}C_{org}$ is the highest (75±18%), followed by that from the IIIa/IIa ratio (58±15%) and then that from the BIT index (43±27%). This difference have been explained by that $\delta^{13}C_{org}$ is a bulk proxy for marine vs. terrestrial influence of sedimentary organic carbon (SOC), whereas the BIT index is for a portion of the bulk SOC, i.e., soil OC (Walsh et al., 2008) or fluvial OC (Sparkes et al., 2015). For the estimated $\%OC_{soil}$, $\delta^{13}C_{org}$ presents a stronger positive correlation with the IIIa/IIa ratio (R^2=0.49) than the BIT index (R^2=0.45), suggesting that the IIIa/IIa ratio may serve a better proxy for quantifying soil organic carbon than the BIT index because it is less affected by selective degradation of branched vs. isoprenoid GDGTs and high production of crenarchaea in marine environments (Smith

et al., 2012).

4 Conclusions

The brGDGTs' distributions in three Bohai Sea cores and globally distributed soils and marine sediments show that the brGDGTs IIIa/IIa ratio is lower than 0.59 in 90% of soils, but higher than 0.92 in 90% of marine sediments, supporting that the IIIa/IIa is a sensitive proxy for assessing soil vs. marine derived brGDGTs at regional and global scales. The in situ production of brGDGTs in marine environments is a ubiquitous phenomenon, which is particularly important for those marine sediments with low BIT index (<0.16) where brGDGTs are exclusively of a marine origin. A systemic difference of the IIIa/IIa value between soils and marine sediments reflects an influence of pH rather than temperature on the biosynthesis of brGDGTs by source organisms. Given these facts, we recommend to calculate the IIIa/IIa ratio before estimating organic carbon source, paleo-soil pH and MAT based on the BIT and MBT/CBT proxies. We also note a relatively large scatter of the IIIa/IIa ratio within terrestrial and marine realms, and recently reported different environmental responses of 5-methyl vs. 6-methyl brGDGTs. As a result, the separation of these two types of isomers is needed in future studies in order to develop more accurate brGDGTs-based proxies.

Acknowledgements. The work was financially supported by the National Science Foundation of China (41476062). We are grateful for X. Dang for GDGT analyses. G. Jia, J. Hu, A. Leider, G. Mollenhauer, G. Trommer and R. Smith are thanked for kindly supplying GDGT data. Dr. Ding He and two anonymous reviewers are thanked for constructive comments.

References

Belicka, L.L., Harvey, H.R., The sequestration of terrestrial organic carbon in Arctic Ocean sediments: A comparison of methods and implications for regional carbon budgets. Geochim. Cosmochim. Acta, 73, 6231–6248, 2009.

411 Blaga, C.I., Reichart, G.J., Vissers, E.W., Lotter, A.F., Anselmetti, F.S., Damste, J.S.S.,
412 Seasonal changes in glycerol dialkyl glycerol tetraether concentrations and
413 fluxes in a perialpine lake: Implications for the use of the TEX_{86} and BIT proxies.
414 Geochim. Cosmochim. Acta, 75, 6416–6428, 2011.
415 Chen, W., Mohtadi, M., Schefuß, E., Mollenhauer, G., Organic-geochemical proxies of
416 sea surface temperature in surface sediments of the tropical eastern Indian
417 Ocean. Deep Sea Research Part I: Oceanographic Research Papers, 88, 17–29,
418 2014.
419 Coffinet, S., Huguet, A., Williamson, D., Fosse, C., Derenne, S., Potential of GDGTs
420 as a temperature proxy along an altitudinal transect at Mount Rungwe
421 (Tanzania). Org. Geochem., 68, 82–89, 2014.
422 De Jonge, C., Hopmans, E.C., Stadnitskaia, A., Rijpstra, W.I.C., Hofland, R., Tegelaar,
423 E., Sinninghe Damsté, J.S., Identification of novel penta- and hexamethylated
424 branched glycerol dialkyl glycerol tetraethers in peat using HPLC–MS2, GC–
425 MS and GC–SMB-MS. Org. Geochem., 54, 78–82, 2013.
426 De Jonge, C., Hopmans, E.C., Zell, C.I., Kim, J.-H., Schouten, S., Sinninghe Damsté,
427 J.S., Occurrence and abundance of 6-methyl branched glycerol dialkyl glycerol
428 tetraethers in soils: Implications for palaeoclimate reconstruction. Geochim.
429 Cosmochim. Acta, 141, 97–112, 2014.
430 De Jonge, C., Stadnitskaia, A., Cherkashov, G., Sinninghe Damsté, J.S., Branched
431 glycerol dialkyl glycerol tetraethers and crenarchaeol record post-glacial sea
432 level rise and shift in source of terrigenous brGDGTs in the Kara Sea (Arctic
433 Ocean). Org. Geochem., 92, 42–54, 2016.
434 De Jonge, C., Stadnitskaia, A., Hopmans, E.C., Cherkashov, G., Fedotov, A.,
435 Streletskaya, I.D., Vasiliev, A.A., Sinninghe Damsté, J.S., Drastic changes in
436 the distribution of branched tetraether lipids in suspended matter and sediments
437 from the Yenisei River and Kara Sea (Siberia): Implications for the use of
438 brGDGT-based proxies in coastal marine sediments. Geochim. Cosmochim.
439 Acta, 165, 200–225, 2015.
440 Ding, S., Xu, Y., Wang, Y., He, Y., Hou, J., Chen, L., He, J.S., Distribution of branched

441 glycerol dialkyl glycerol tetraethers in surface soils of the Qinghai–Tibetan
442 Plateau: implications of brGDGTs-based proxies in cold and dry regions.
443 Biogeosciences, 12, 3141–3151, 2015.
444 Dong, L., Li, Q., Li, L., Zhang, C.L., Glacial–interglacial contrast in MBT/CBT proxies
445 in the South China Sea: Implications for marine production of branched GDGTs
446 and continental teleconnection. Org. Geochem., 79, 74–82, 2015.
447 Fietz, S., Huguet, C., Bendle, J., Escala, M., Gallacher, C., Herfort, L., Jamieson, R.,
448 Martínez-Garcia, A., McClymont, E.L., Peck, V.L., Prahl, F.G., Rossi, S., Rueda,
449 G., Sanson-Barrera, A., Rosell-Melé, A., Co-variation of crenarchaeol and
450 branched GDGTs in globally-distributed marine and freshwater sedimentary
451 archives. Glob. Planet. Change, 92, 275–285, 2012.
452 Fietz, S., Prahl, F.G., Moraleda, N., Rosell-Melé, A., Eolian transport of glycerol
453 dialkyl glycerol tetraethers (GDGTs) off northwest Africa. Org. Geochem., 64,
454 112–118, 2013.
455 French, D.W., Huguet, C., Turich, C., Wakeham, S.G., Carlson, L.T., Ingalls, A.E.,
456 Spatial distributions of core and intact glycerol dialkyl glycerol tetraethers
457 (GDGTs) in the Columbia River Basin and Willapa Bay, Washington: Insights
458 into origin and implications for the BIT index. Org. Geochem., 88, 91–112,
459 2015.
460 Herfort, L., Schouten, S., Boon, J.P., Woltering, M., Baas, M., Weijers, J.W.H., Damsté,
461 J.S.S., Characterization of transport and deposition of terrestrial organic matter
462 in the southern North Sea using the BIT index. Limnol. Oceanogr., 51, 2196 –
463 2205, 2006.
464 Hopmans, E.C., Weijers, J.W.H., Schefuss, E., Herfort, L., Damste, J.S.S., Schouten, S.,
465 A novel proxy for terrestrial organic matter in sediments based on branched and
466 isoprenoid tetraether lipids. Earth Planet. Sci. Lett., 224, 107–116, 2004.
467 Hu, J., Meyers, P.A., Chen, G., Peng, P.A., Yang, Q., Archaeal and bacterial glycerol
468 dialkyl glycerol tetraethers in sediments from the Eastern Lau Spreading Center,
469 South Pacific Ocean. Org. Geochem., 43, 162–167, 2012.
470 Hu, J., Zhou, H., Peng, P.A., Spiro, B., Seasonal variability in concentrations and fluxes

of glycerol dialkyl glycerol tetraethers in Huguangyan Maar Lake, SE China: Implications for the applicability of the MBT–CBT paleotemperature proxy in lacustrine settings. Chem. Geol., 420, 200 – 212, 2016.

Hu, L., Guo, Z., Feng, J., Yang, Z., Fang, M., Distributions and sources of bulk organic matter and aliphatic hydrocarbons in surface sediments of the Bohai Sea, China. Mar. Chem., 113, 197–211, 2009.

Huguet, A., Fosse, C., Metzger, P., Fritsch, E., Derenne, S., Occurrence and distribution of extractable glycerol dialkyl glycerol tetraethers in podzols. Org. Geochem., 41, 291–301, 2010.

Huguet, C., de Lange, G.J., Gustafsson, Ö., Middelburg, J.J., Sinninghe Damsté, J.S., Schouten, S., Selective preservation of soil organic matter in oxidized marine sediments (Madeira Abyssal Plain). Geochim. Cosmochim. Acta, 72, 6061–6068, 2008.

Huguet, C., Kim, J.-H., de Lange, G.J., Sinninghe Damsté, J.S., Schouten, S., Effects of long term oxic degradation on the , TEX_{86} and BIT organic proxies. Org. Geochem., 40, 1188–1194, 2009.

Jia, G., Zhang, J., Chen, J., Peng, P.A., Zhang, C.L., Archaeal tetraether lipids record subsurface water temperature in the South China Sea. Org. Geochem., 50, 68–77, 2012.

Kaiser, J., Schouten, S., Kilian, R., Arz, H.W., Lamy, F., Sinninghe Damsté, J.S., Isoprenoid and branched GDGT-based proxies for surface sediments from marine, fjord and lake environments in Chile. Org. Geochem., 89, 117–127, 2015.

Kim, J.-H., Schouten, S., Rodrigo-Gámiz, M., Rampen, S., Marino, G., Huguet, C., Helmke, P., Buscail, R., Hopmans, E.C., Pross, J., Sangiorgi, F., Middelburg, J.B.M., Sinninghe Damsté, J.S., Influence of deep-water derived isoprenoid tetraether lipids on the paleothermometer in the Mediterranean Sea. Geochim. Cosmochim. Acta, 150, 125–141, 2015.

Kim, J.H., Meer, J.V.D., Schouten, S., Helmke, P., Willmott, V., Sangiorgi, F., Koç, N., Hopmans, E.C., Damsté, J.S.S., New indices and calibrations derived from the

501 distribution of crenarchaeal isoprenoid tetraether lipids: Implications for past
502 sea surface temperature reconstructions. Geochim. Cosmochim. Acta, 74,
503 4639–4654, 2010.
504 Kim, J.H., Schouten, S., Buscail, R., Ludwig, W., Bonnin, J., Sinninghe Damsté, J.S.,
505 Bourrin, F., Origin and distribution of terrestrial organic matter in the NW
506 Mediterranean (Gulf of Lions): Exploring the newly developed BIT index.
507 Geochem. Geophy. Geosy., 7, 220–222, 2006.
508 Leider, A., Hinrichs, K.U., Mollenhauer, G., Versteegh, G.J.M., Core-top calibration of
509 the lipid-based UK'37 and TEX_{86} temperature proxies on the southern Italian
510 shelf (SW Adriatic Sea, Gulf of Taranto). Earth Planet. Sci. Lett., 300, 112–124,
511 2010.
512 Lincoln, S.A., Wai, B., Eppley, J.M., Church, M.J., Summons, R.E., Delong, E.F.,
513 Planktonic Euryarchaeota are a significant source of archaeal tetraether lipids
514 in the ocean. Proc. Natl. Acad. Sci., 111, 9858–9863, 2014.
515 Lipp, J.S., Morono, Y., Inagaki, F., Hinrichs, K.U., Significant contribution of Archaea
516 to extant biomass in marine subsurface sediments. Nature, 454, 991–994, 2008.
517 Liu, X.-L., Zhu, C., Wakeham, S.G., Hinrichs, K.-U., In situ production of branched
518 glycerol dialkyl glycerol tetraethers in anoxic marine water columns. Mar.
519 Chem., 166, 1–8, 2014.
520 Loomis, S.E., Russell, J.M., Damsté, J.S.S., Distributions of branched GDGTs in soils
521 and lake sediments from western Uganda: Implications for a lacustrine
522 paleothermometer. Org. Geochem., 42, 739–751, 2011.
523 Meyers, P.A., Organic geochemical proxies of paleoceanographic, paleolimnologic,
524 and paleoclimatic processes. Org. Geochem., 27, 213–250, 1997.
525 Milliman, J.D., Meade, R.H., World-wide delivery of river sediment to the oceans. J.
526 Geol., 91, 1–21, 1983.
527 Mueller-Niggemann, C., Utami, S.R., Marxen, A., Mangelsdorf, K., Bauersachs, T.,
528 Schwark, L., Distribution of tetraether lipids in agricultural soils–differentiation
529 between paddy and upland management. Biogeosciences, 13, 1647–1666, 2016.
530 O'Brien, C.L., Foster, G.L., Martínez-Botí, M.A., Abell, R., Rae, J.W.B., Pancost, R.D.,

531 High sea surface temperatures in tropical warm pools during the Pliocene. Nat
532 Geosci, 7, 606–611, 2014.
533 Peterse, F., Kim, J.-H., Schouten, S., Kristensen, D.K., Koç, N., Sinninghe Damsté, J.S.,
534 Constraints on the application of the MBT/CBT palaeothermometer at high
535 latitude environments (Svalbard, Norway). Org. Geochem., 40, 692–699, 2009a.
536 Peterse, F., Schouten, S., van der Meer, J., van der Meer, M.T.J., Sinninghe Damsté,
537 J.S., Distribution of branched tetraether lipids in geothermally heated soils:
538 Implications for the MBT/CBT temperature proxy. Org. Geochem., 40, 201–
539 205, 2009b.
540 Peterse, F., van der Meer, J., Schouten, S., Weijers, J.W.H., Fierer, N., Jackson, R.B.,
541 Kim, J.-H., Sinninghe Damsté, J.S., Revised calibration of the MBT–CBT
542 paleotemperature proxy based on branched tetraether membrane lipids in
543 surface soils. Geochim. Cosmochim. Acta, 96, 215–229, 2012.
544 Peterse, F., Vonk, J.E., Holmes, R.M., Giosan, L., Zimov, N., Eglinton, T.I., Branched
545 glycerol dialkyl glycerol tetraethers in Arctic lake sediments: Sources and
546 implications for paleothermometry at high latitudes. J. Geophys. Res.-Biogeo.,
547 119, 1738–1754, 2014.
548 Ren, M.-E., Shi, Y.-L., Sediment discharge of the Yellow River (China) and its effect
549 on the sedimentation of the Bohai and the Yellow Sea. Cont. Shelf. Res., 6, 785–
550 810, 1986.
551 Schouten, S., Hopmans, E.C., Baas, M., Boumann, H., Standfest, S., Konneke, M.,
552 Stahl, D.A., Sinninghe Damste, J.S., Intact membrane lipids of "Candidatus
553 Nitrosopumilus maritimus," a cultivated representative of the cosmopolitan
554 mesophilic group I Crenarchaeota. Appl. Environ. Microbiol., 74, 2433–2440,
555 2008.
556 Schouten, S., Hopmans, E.C., Schefuß, E., Sinninghe Damsté, J.S., Distributional
557 variations in marine crenarchaeotal membrane lipids: a new tool for
558 reconstructing ancient sea water temperatures? Earth Planet. Sci. Lett., 204,
559 265–274, 2002.
560 Schouten, S., Hopmans, E.C., Sinninghe Damsté, J.S., The organic geochemistry of

glycerol dialkyl glycerol tetraether lipids: A review. Org. Geochem., 54, 19–61, 2013.

Sinninghe Damsté, J.S., Spatial heterogeneity of sources of branched tetraethers in shelf systems: The geochemistry of tetraethers in the Berau River delta (Kalimantan, Indonesia). Geochim. Cosmochim. Acta, 186, 13–31, 2016.

Sinninghe Damsté, J.S., Hopmans, E.C., Pancost, R.D., Schouten, S., Geenevasen, J.A.J., Newly discovered non-isoprenoid glycerol dialkyl glycerol tetraether lipids in sediments. Chem. Commun., 17, 1683–1684, 2000.

Sinninghe Damsté, J.S., Ossebaar, J., Abbas, B., Schouten, S., Verschuren, D., Fluxes and distribution of tetraether lipids in an equatorial African lake: Constraints on the application of the TEX_{86} palaeothermometer and BIT index in lacustrine settings. Geochim. Cosmochim. Acta, 73, 4232–4249, 2009.

Sinninghe Damsté, J.S., Ossebaar, J., Schouten, S., Verschuren, D., Altitudinal shifts in the branched tetraether lipid distribution in soil from Mt. Kilimanjaro (Tanzania): Implications for the MBT/CBT continental palaeothermometer. Org. Geochem., 39, 1072–1076, 2008.

Sinninghe Damsté, J.S., Rijpstra, W.I.C., Hopmans, E.C., Weijers, J.W.H., Foesel, B.U., Overmann, J., Dedysh, S.N., 13,16-Dimethyl Octacosanedioic Acid (iso-Diabolic Acid), a Common Membrane-Spanning Lipid of Acidobacteria Subdivisions 1 and 3. Appl. Environ. Microbiol., 77, 4147–4154, 2011.

Sinninghe Damsté, J.S., Schouten, S., Hopmans, E.C., van Duin, A.C.T., Geenevasen, J.A.J., Crenarchaeol: the characteristic core glycerol dibiphytanyl glycerol tetraether membrane lipid of cosmopolitan pelagic crenarchaeota. J. Lipid Res., 43, 1641–1651, 2002.

Smith, R.W., Bianchi, T.S., Li, X., A re-evaluation of the use of branched GDGTs as terrestrial biomarkers: Implications for the BIT Index. Geochim. Cosmochim. Acta, 80, 14–29, 2012.

Sofianos, S.S., Johns, W.E., Murray, S.P., Heat and freshwater budgets in the Red Sea from direct observations at Bab el Mandeb. Deep Sea Res. Part II: Top. Stud. Oceanogr., 49, 1323–1340, 2002.

591 Sparkes, R.B., Doğrul Selver, A., Bischoff, J., Talbot, H.M., Gustafsson, Ö., Semiletov,
592 I.P., Dudarev, O.V., van Dongen, B.E., GDGT distributions on the East Siberian
593 Arctic Shelf: implications for organic carbon export, burial and degradation.
594 Biogeosciences, 12, 3753–3768, 2015.
595 Taylor, K.W.R., Huber, M., Hollis, C.J., Hernandez-Sanchez, M.T., Pancost, R.D., Re-
596 evaluating modern and Palaeogene GDGT distributions: Implications for SST
597 reconstructions. Glob. Planet. Change, 108, 158–174, 2013.
598 Tierney, J.E., Russell, J.M., Distributions of branched GDGTs in a tropical lake system:
599 Implications for lacustrine application of the MBT/CBT paleoproxy. Org.
600 Geochem., 40, 1032–1036, 2009.
601 Tierney, J.E., Schouten, S., Pitcher, A., Hopmans, E.C., Sinninghe Damsté, J.S., Core
602 and intact polar glycerol dialkyl glycerol tetraethers (GDGTs) in Sand Pond,
603 Warwick, Rhode Island (USA): Insights into the origin of lacustrine GDGTs.
604 Geochim. Cosmochim. Acta, 77, 561–581, 2012.
605 Trommer, G., Siccha, M., Meer, M.T.J.V.D., Schouten, S., Damsté, J.S.S., Schulz, H.,
606 Hemleben, C., Kucera, M., Distribution of Crenarchaeota tetraether membrane
607 lipids in surface sediments from the Red Sea. Org. Geochem., 40, 724–731,
608 2009.
609 Walsh, E.M., Ingalls, A.E., Keil, R.G., Sources and transport of terrestrial organic
610 matter in Vancouver Island fjords and the Vancouver-Washington Margin: A
611 multiproxy approach using d13Corg, lignin phenols, and the ether lipid BIT
612 index. Limnol. Oceanogr., 53, 1054–1063, 2008.
613 Weijers, J.W.H., Schefuß, E., Kim, J.-H., Sinninghe Damsté, J.S., Schouten, S.,
614 Constraints on the sources of branched tetraether membrane lipids in distal
615 marine sediments. Org. Geochem., 72, 14–22, 2014.
616 Weijers, J.W.H., Schefuß, E., Schouten, S., Damsté, J.S.S., Coupled thermal and
617 hydrological evolution of tropical Africa over the last deglaciation. Science, 315,
618 1701–1704, 2007a.
619 Weijers, J.W.H., Schouten, S., Donker, J.C.V.D., Hopmans, E.C., Damsté, J.S.S.,
620 Environmental controls on bacterial tetraether membrane lipid distribution in

621 soils. Geochim. Cosmochim. Acta, 71, 703–713, 2007b.
622 Weijers, J.W.H., Schouten, S., Spaargaren, O.C., Sinninghe Damsté, J.S., Occurrence
623 and distribution of tetraether membrane lipids in soils: Implications for the use
624 of the TEX_{86} proxy and the BIT index. Org. Geochem., 37, 1680–1693, 2006.
625 White, D.C., Davis, W.M., Nickels, J.S., King, J.D., Bobbie, R.J., Determination of the
626 sedimentary microbial biomass by extractible lipid phosphate. Oecologia, 40,
627 51–62, 1979.
628 Wu, W., Ruan, J., Ding, S., Zhao, L., Xu, Y., Yang, H., Ding, W., Pei, Y., Source and
629 distribution of glycerol dialkyl glycerol tetraethers along lower Yellow River-
630 estuary–coast transect. Mar. Chem., 158, 17–26, 2014.
631 Wu, W., Zhao, L., Pei, Y., Ding, W., Yang, H., Xu, Y., Variability of tetraether lipids in
632 Yellow River-dominated continental margin during the past eight decades:
633 Implications for organic matter sources and river channel shifts. Org. Geochem.,
634 60, 33–39, 2013.
635 Xiao, W., Xu, Y., Ding, S., Wang, Y., Zhang, X., Yang, H., Wang, G., Hou, J., Global
636 calibration of a novel, branched GDGT-based soil pH proxy. Org. Geochem.,
637 89, 56–60, 2015.
638 Yang, G., Zhang, C.L., Xie, S., Chen, Z., Gao, M., Ge, Z., Yang, Z., Microbial glycerol
639 dialkyl glycerol tetraethers lipids from water and soil at the Three Gorges Dam
640 on the Yangtze River. Org. Geochem., 56, 40–50, 2013.
641 Yang, H., Pancost, R.D., Dang, X., Zhou, X., Evershed, R.P., Xiao, G., Tang, C., Gao,
642 L., Guo, Z., Xie, S., Correlations between microbial tetraether lipids and
643 environmental variables in Chinese soils: Optimizing the paleo-reconstructions
644 in semi-arid and arid regions. Geochim. Cosmochim. Acta, 126, 49–69, 2014a.
645 Yang, H., Pancost, R.D., Tang, C., Ding, W., Dang, X., Xie, S., Distributions of
646 isoprenoid and branched glycerol dialkanol diethers in Chinese surface soils and
647 a loess–paleosol sequence: Implications for the degradation of tetraether lipids.
648 Org. Geochem., 66, 70-79, 2014b.
649 Zell, C., Kim, J.-H., Dorhout, D., Baas, M., Sinninghe Damsté, J.S., Sources and
650 distributions of branched tetraether lipids and crenarchaeol along the

Portuguese continental margin: Implications for the BIT index. Cont. Shelf. Res., 96, 34–44, 2015.

Zell, C., Kim, J.-H., Hollander, D., Lorenzoni, L., Baker, P., Silva, C.G., Nittrouer, C., Sinninghe Damsté, J.S., Sources and distributions of branched and isoprenoid tetraether lipids on the Amazon shelf and fan: Implications for the use of GDGT-based proxies in marine sediments. Geochim. Cosmochim. Acta, 139, 293–312, 2014.

Zhang, Y.G., Zhang, C.L., Liu, X.-L., Li, L., Hinrichs, K.-U., Noakes, J.E., Methane Index: A tetraether archaeal lipid biomarker indicator for detecting the instability of marine gas hydrates. Earth Planet. Sci. Lett., 307, 525-534, 2011.

Zhu, C., Wakeham, S.G., Elling, F.J., Basse, A., Mollenhauer, G., Versteegh, G.J.M., ouml, nneke, M., Hinrichs, K.U., Stratification of archaeal membrane lipids in the ocean and implications for adaptation and chemotaxonomy of planktonic archaea. Environ. Microbiol., DOI: 10.1111/1462-2920.13289, 2016.

Zhu, C., Weijers, J.W.H., Wagner, T., Pan, J.M., Chen, J.F., Pancost, R.D., Sources and distributions of tetraether lipids in surface sediments across a large river-dominated continental margin. Org. Geochem., 42, 376–386, 2011.

Fig.1. Chemical structures of branched GDGTs and crenarchaeol.

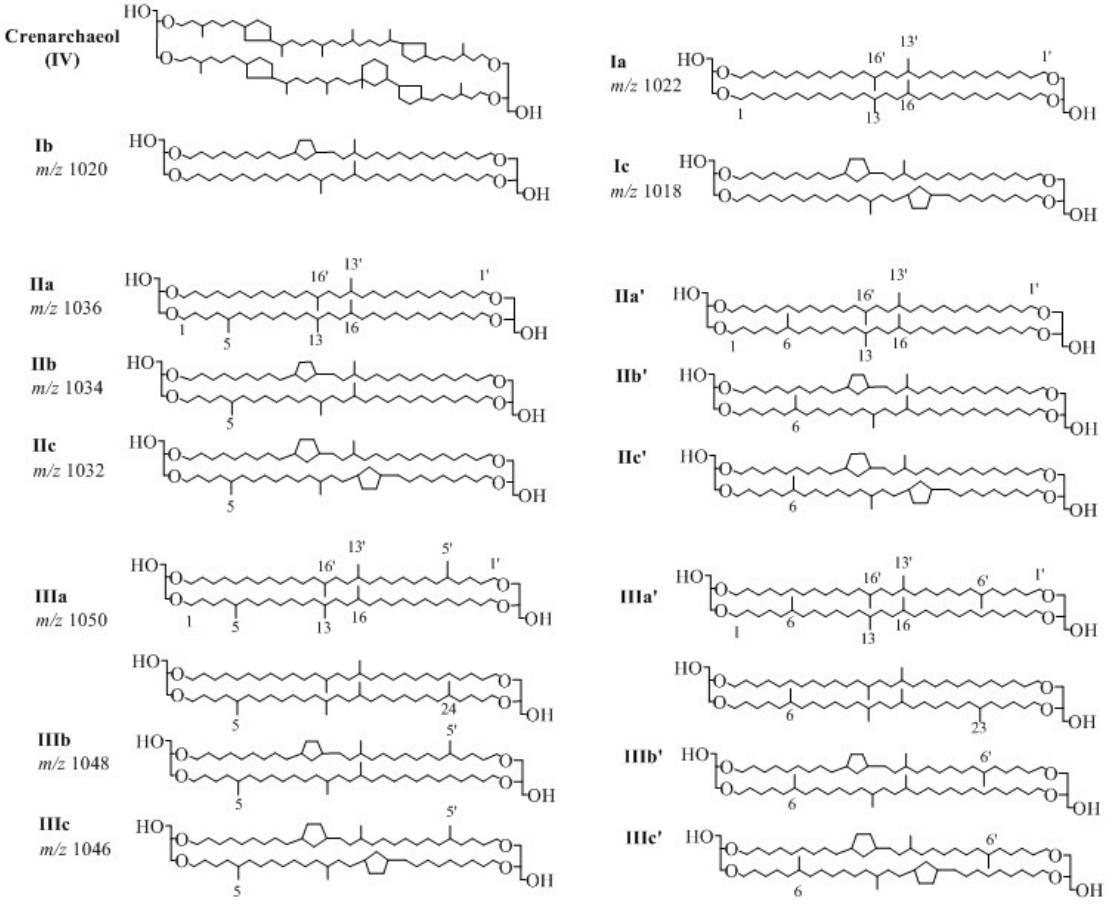

Fig.2. Location of the samples used in this study. White circles and black circles indicate the soils and marine sediments, respectively. Red crosses denote three sediment cores (M1, M3 and M7) in the Bohai Sea. YR is the Yellow River.

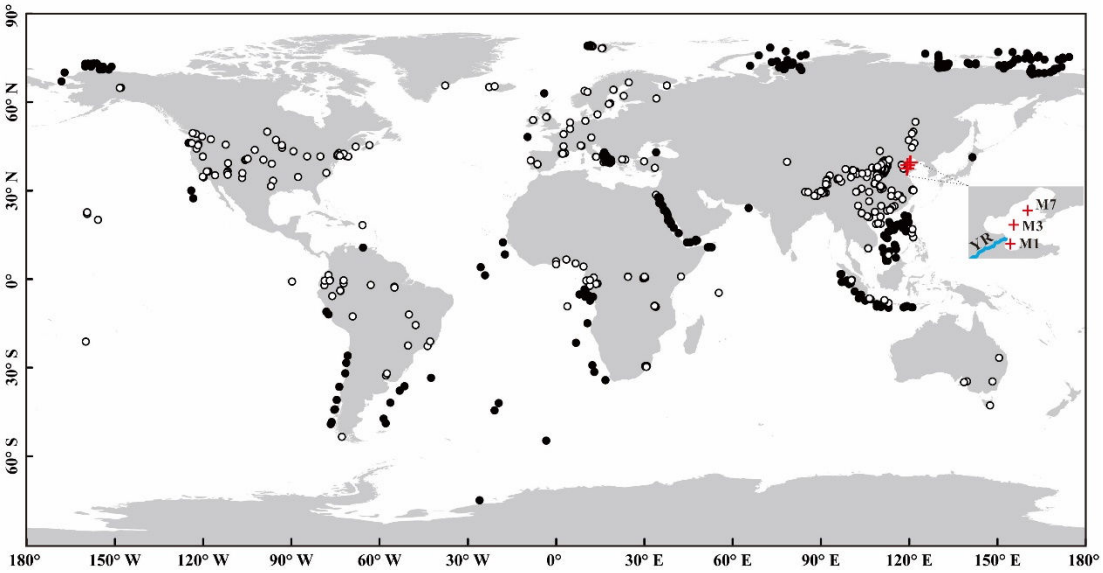

Fig.3. Averaged percentages of individual brGDGTs in soils (a), core M1 (b), M3 (c) and M7 (d). The soil data are from Yang et al. (2014a).

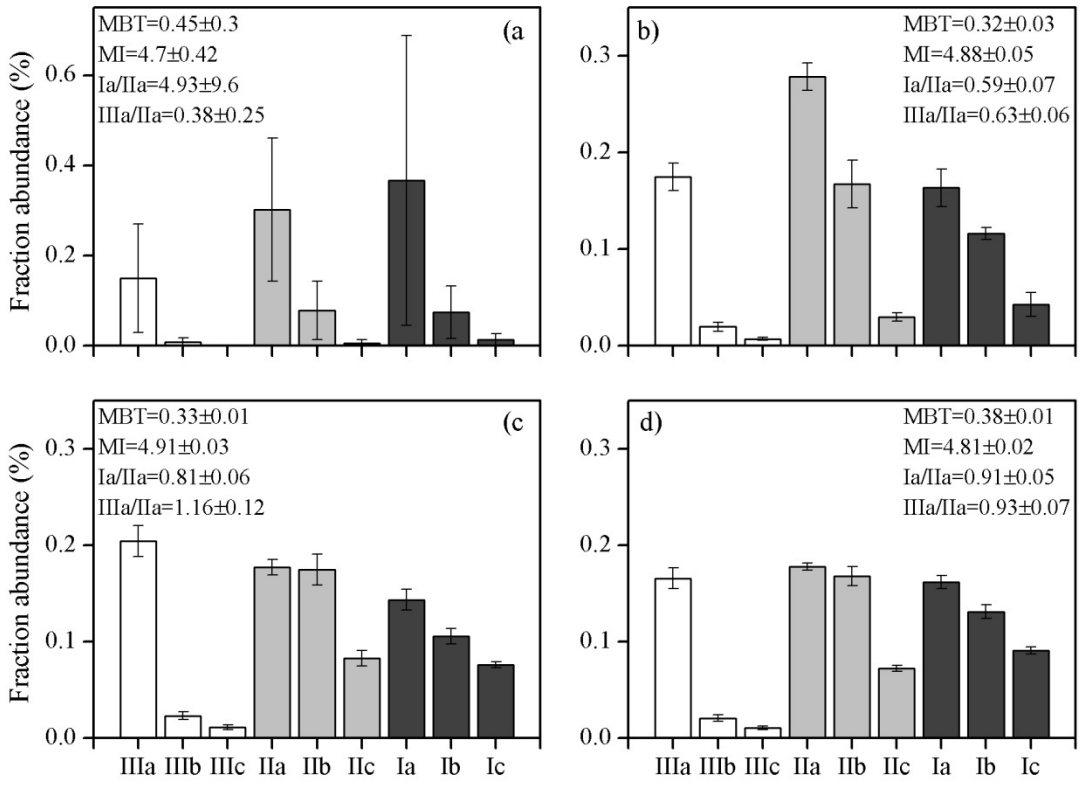

Fig. 4. a) The relationship between brGDGT IIIa/IIa ratio and the BIT index of samples from Peterse et al. (2009a); b) histograms of brGDGT IIIa/IIa ratio of the core lipids (CLs) and intact polar lipids (IPLs) in samples from De Jonge et al. (2015); c) the relationship between brGDGT IIIa/IIa ratio and the BIT index in samples from Sparkes et al. (2015); d) the relationship between brGDGT IIIa/IIa ratio and distance from river mouth in samples from Sparkes et al. (2015).

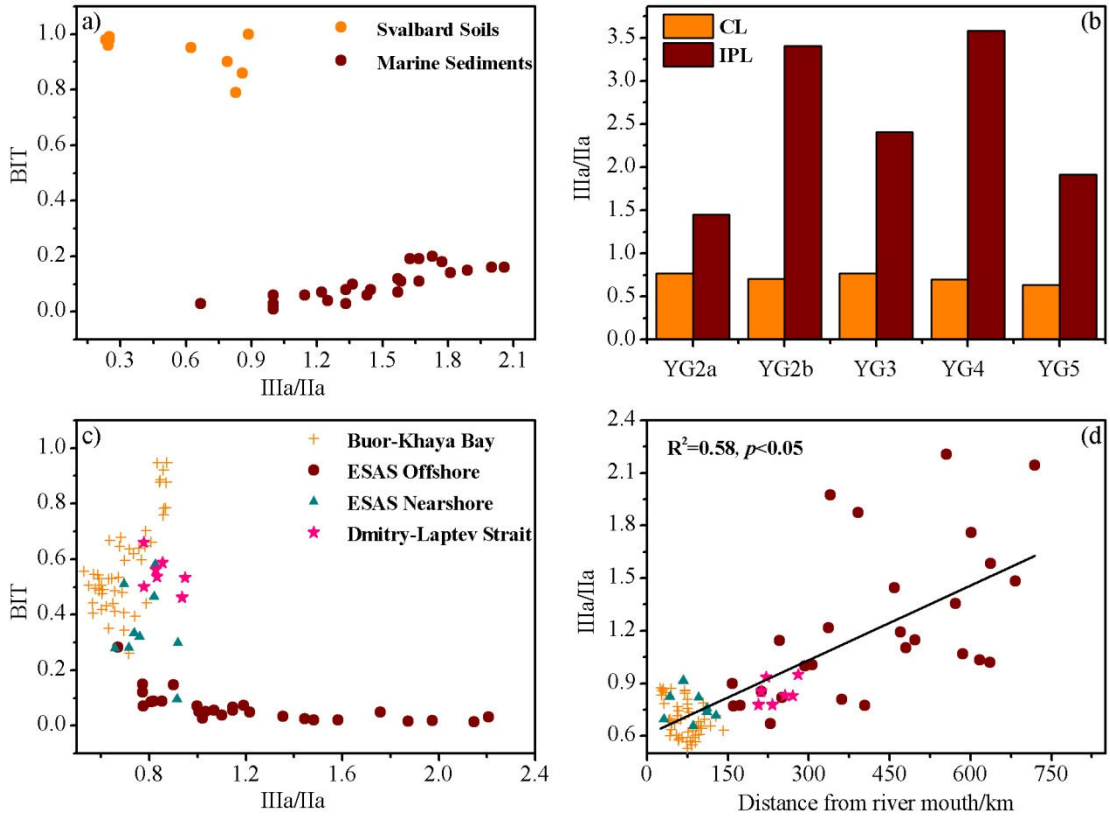

Fig. 5. Global distribution pattern of brGDGT IIIa/IIa ratio in soils and marine sediments.

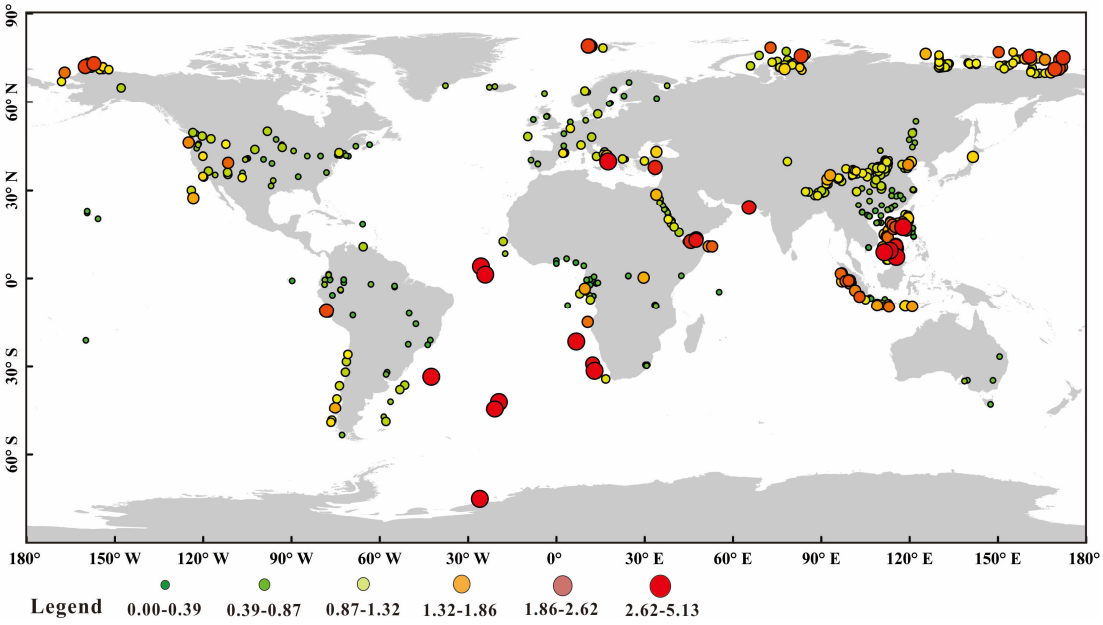

773 Fig. 6 a plot showing a positive correlation between soil pH and IIIa/IIa. The data are from
774 Peterse et al. (2012) and this study.

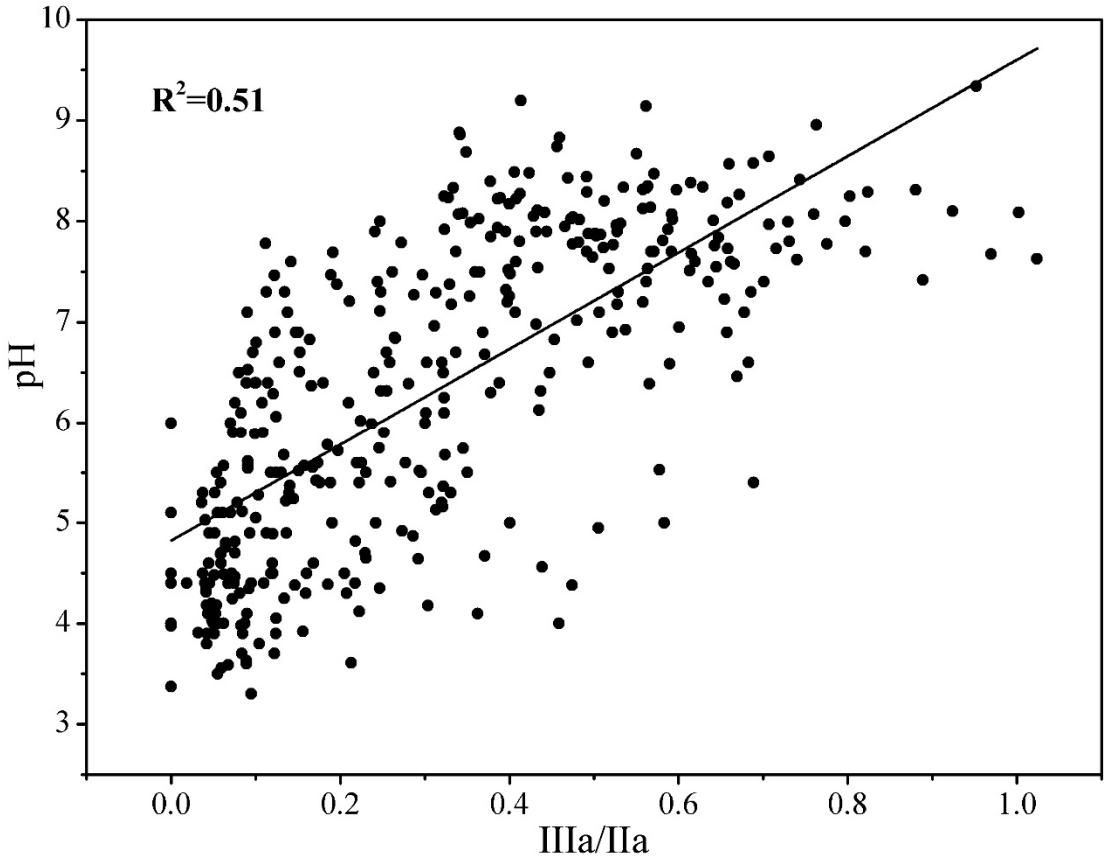

775
776
777
778
779
780
781
782
783
784
785
786
787
788
789

Fig. 7. Relationship between the IIIa/IIa ratio and the BIT index of globally distributed samples: soils (orange circle) and marine sediments (red circle). Dashed lines represent lower or upper threshold values for 90% of soils/sediments.

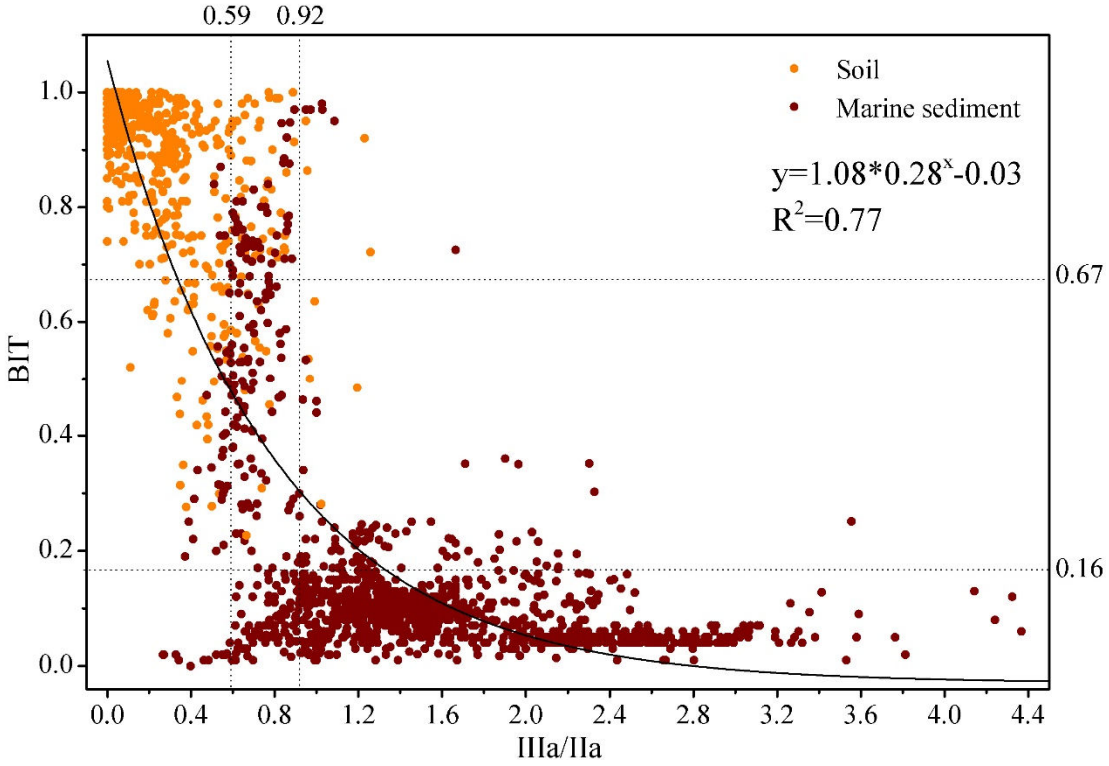

Fig. 8. Percentage of soil organic carbon ($\%OC_{soil}$) or terrestrial organic carbon ($\%OC_{terr}$) based on a binary mixing model of BIT (a), $\delta^{13}C_{org}$ (b) and IIIa/IIa (c) for the East Siberian Arctic Shelf (Sparkes et al., 2015).

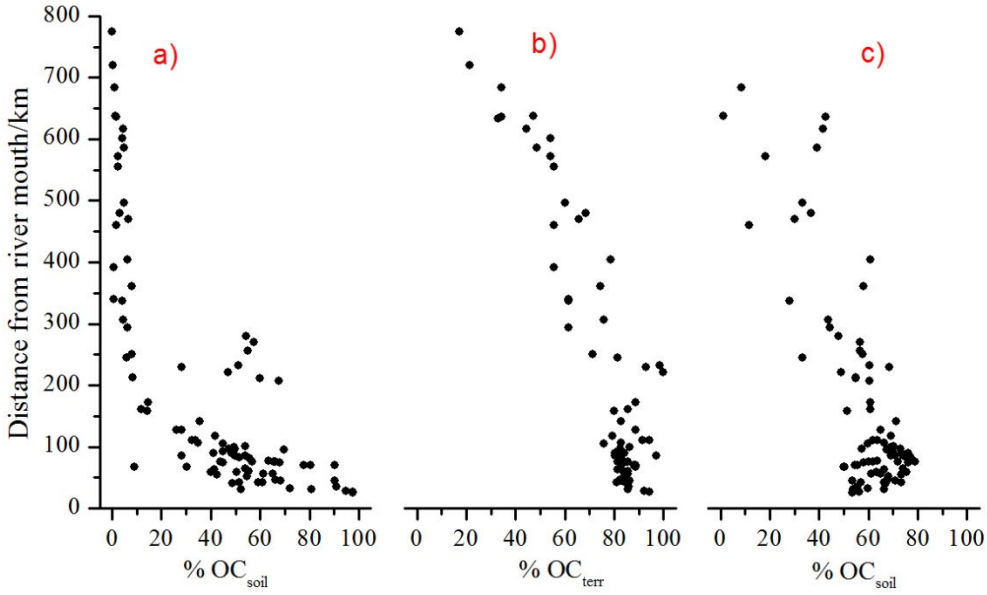

829 Table 1: Parameters including brGDGTs IIIa/IIa, Ia/IIa, the BIT index, MBT, MI, DC,
830 percentages of tetra-, penta- and hexa-methylated brGDGTs, and the weighted average
831 number of cyclopentane moieties (#rings for tetramethylated brGDGTs) based on the
832 GDGTs from three cores (M1, M3 and M7; see figure 2) in the Bohai Sea. Different
833 letters in parentheses (a, b, c, d) represent significant difference at the level of $p<0.05$.

Indexes	Soil	M1	M3	M7
IIIa/IIa	0.39±0.25 (a)	0.63±0.06 (b)	1.16±0.12 (c)	0.93±0.07 (d)
Ia/IIa	4.93±9.60 (a)	0.59±0.07 (b)	0.81±0.06 (b)	0.91±0.05 (b)
BIT	0.75±0.22 (a)	0.50±0.19 (b)	0.14±0.06 (c)	0.11±0.03 (c)
MBT	0.45±0.30 (a)	0.32±0.03 (b)	0.33±0.01 (b)	0.38±0.01 (ab)
MI	4.70±0.42 (a)	4.88±0.05 (b)	4.91±0.03 (b)	4.81±0.02 (ab)
DC	0.31±0.21 (a)	0.62±0.03 (b)	0.79±0.03 (c)	0.82±0.02 (c)
%tetra	0.45±0.30 (a)	0.32±0.03 (b)	0.33±0.01 (c)	0.38±0.01 (c)
%hexa	0.16±0.12 (a)	0.20±0.02 (b)	0.24±0.02 (b)	0.20±0.01 (b)
%penta	0.39±0.20 (a)	0.48±0.02 (b)	0.44±0.02 (b)	0.42±0.01 (b)
$\#Rings_{tera}$	0.20±0.15 (a)	0.39±0.03 (b)	0.47±0.02 (c)	0.47±0.02 (c)

834

835